# High resolution $\delta^{13}C$ stratigraphy of the Homerian (Wenlock) of the English Midlands and Wenlock Edge

CARLY MARSHALL, ALAN T. THOMAS, IAN BOOMER & DAVID C. RAY

High resolution $\delta^{13}C_{carb}$ data are presented for two composite sections in England covering much of the Homerian Stage. Micrite samples collected at ~0.5 m intervals from outcrop and core in the Dudley area, West Midlands, span the uppermost Coalbrookdale, Much Wenlock Limestone and basal Lower Elton formations. Deposition there occurred in a mid-shelf setting. A similar suite of samples from the Wenlock type area, Wenlock Edge, Shropshire, represents a coeval sequence deposited closer to the shelf-basin margin. The successions concerned extend from the upper *lundgreni* to *nilssoni* graptolite biozones and provide a detailed record of variation in stable carbon isotope ratios across the well-known double-peaked Homerian positive excursion (Mulde Excursion), a time of significant global biological and chemical perturbation. In the West Midlands, this excursion occurs in the Much Wenlock Limestone Formation. The lower peak (Lower Quarried Limestone Member) has $\delta^{13}C_{carb}$ values rising to +5.5‰ VPDB. Values fall to +0.8‰ VPDB higher in the section before rising again to +4.1‰ VPDB (Nodular Beds Member). Analysis of lithofacies variation in this interval indicates two transgressive-regressive cycles, the two positive peaks of the excursion correlating with relative sea-level lows and the intervening dip with a relative sea-level high, the local expression of Johnson's (2006) Highstand 5A. The double-peaked nature of the excursion at Dudley resembles that previously recorded for the area; however, our $\delta^{13}C_{carb}$ values are consistently 2‰ higher, and accord more closely with values published for sections elsewhere. The lower of the two peaks found in the West Midlands cannot be identified on Wenlock Edge, where $\delta^{13}C_{carb}$ values fluctuate somewhat around +2‰ VPDB. The upper peak, though less distinct, can be identified on Wenlock Edge with values rising to +3.8‰ VPDB. Correlations based on biostratigraphy, sequence stratigraphy and bentonite geochemistry suggest that not all changes in $\delta^{13}C_{carb}$ occurred synchronously in the two areas studied, despite their close proximity. • Key words: Silurian, Wenlock, Homerian, $\delta^{13}C$ stratigraphy, Mulde Excursion, English Midlands.

MARSHALL, C., THOMAS, A.T., BOOMER, I. & RAY, D.C. 2012. High resolution $\delta^{13}C$ stratigraphy of the Homerian (Wenlock) of the English Midlands and Wenlock Edge. *Bulletin of Geosciences 87(4)*, 669–679 (2 figures, 2 appendices). Czech Geological Survey, Prague. ISSN 1214-1119. Manuscript received July 31, 2011; accepted in revised form May 30, 2012; published online October 17, 2012; issued October 17, 2012.

*Carly Marshall (corresponding author), Alan T. Thomas & Ian Boomer, Geosystems Research Group, School of Geography, Earth and Environmental Sciences, University of Birmingham, Birmingham, B15 2TT, UK, present address: VNG Norge AS. Postboks 720 Sentrum, NO-4003 Stavanger, Norway; Carly.Marshall@vng.no • Alan T. Thomas & Ian Boomer, Geosystems Research Group, School of Geography, Earth and Environmental Sciences, University of Birmingham, Birmingham, B15 2TT, UK • David C. Ray, Neftex Petroleum Consultants Ltd, 97 Milton Park, Abingdon, Oxfordshire, OX14 4RY, UK*

Traditionally viewed as a period of stable greenhouse climates, the Silurian is now recognised as a time of significant environmental variation (Calner 2008, Munnecke *et al.* 2010), associated with pronounced atmospheric, biotic and oceanic change, in part linked to Gondwanan glaciations (Grahn & Caputo 1992, Johnson 2006, Melchin & Holmden 2006, Calner 2008). Analysis of the inorganic carbon isotopic composition of Silurian limestones ($\delta^{13}C_{carb}$) provides data that contribute to identifying and understanding these variations, although the causal mechanisms linking atmospheric, biotic, oceanic and $\delta^{13}C$ changes remain controversial (Calner 2008). Temporal variations in carbon isotope composition have potential as a tool for international correlation also, although our data reveal some inconsistencies when detailed correlations using carbon isotopes, biostratigraphy, sequence stratigraphy and geochemical data from bentonites are compared. Excellent outcrops of well-preserved limestones spanning much of the upper Wenlock Homerian Stage occur widely in the English Midlands and Welsh borderlands (see Fig. 1 for localities and palaeogeography). This paper presents high resolution $\delta^{13}C_{carb}$ data from two composite sections spanning much of the stage, including the Homerian type area, and discusses inconsistencies that arise in detailed correlation.

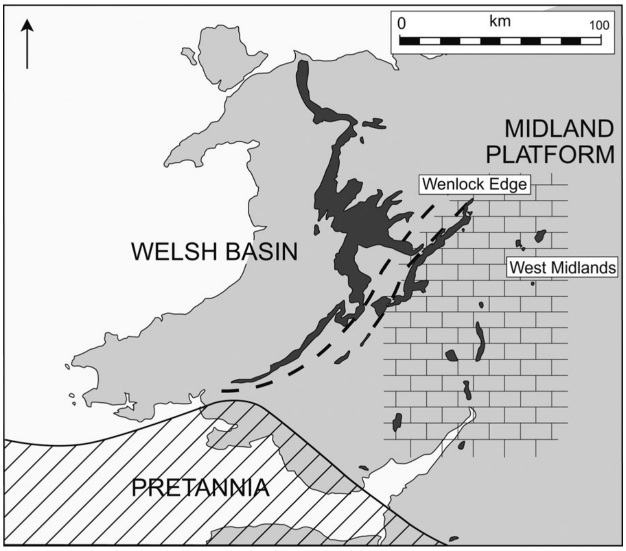


**Figure 1.** Map of England and adjacent parts of Wales showing key elements of palaeogeography in late Wenlock times; the positions of Wenlock Edge and the West Midlands are shown. Dark grey areas represent Wenlock outcrop; broken lines represent the major elements of the Welsh Borderland Fault System that controlled the local basin/shelf boundary. Brick-like ornament represents outcrop area of the Much Wenlock Limestone Formation and diagonal ornamentation denotes land.

## Methods

Micrite samples from the uppermost Coalbrookdale, Much Wenlock Limestone and basal Lower Elton formations (for lithostratigraphy see Fig. 2) were collected at approximately 0.5 m intervals from a limestone mine, a borehole core and surface outcrops in the Dudley area, West Midlands (Stepshaft Mine, Mons Hill core and Wren's Nest Inlier). A near coeval set of samples was collected from outcrops along Wenlock Edge, Shropshire (Lower Hill Farm Track, Acklands Coppice, Farley Road Cutting, Harley Hill, Lea South Quarry). Both sections are considered to span the upper *lundgreni* to *nilissoni* biozones, but are associated with mid-shelf and shelf–basin-margin settings respectively (Fig. 1; Ratcliffe & Thomas 1999).

The stable carbon and oxygen isotope compositions of nearly 300 samples were determined. Micrite samples (200 μg) were powdered, placed into 4 ml glass vials and sealed by a lid and pierceable septum. The vials were put in a heated sample rack (90 °C) where the vial head space was replaced by pure helium via an automated needle system as part of a GV Instruments Multiflow preparation system. Samples were then manually injected with approximately 100 μl of phosphoric acid and left to react for 1 hour before the head space gas was automatically sampled by needle and introduced into a continuous-flow GV Isoprime mass-spectrometer. Samples were calibrated using IAEA standards CO-1 and CO-8. Analytical precision based on duplicate analyses is generally better than 0.1‰ for both $\delta^{13}C$ and $\delta^{18}O$. A complete listing of the isotope results is provided in the appendix.

## Stratigraphical framework

The Much Wenlock Limestone Formation is internationally renowned for its prolific and diverse skeletal biota, particularly in the West Midlands (see Thomas 1978; Ratcliffe 1991, 1999; Aldridge *et al.* 2000; Ray & Thomas 2007 for summary reviews). It has been the subject of extensive sedimentological and palaeoenvironmental study also (Scoffin 1971, Ratcliffe & Thomas 1999). Some aspects of the formation's stratigraphy have remained contentious however, in particular the exact details of the correlation between the West Midlands and Wenlock Edge and the extent to which the lower and upper boundaries of the formation may be diachronous (Bassett 1974, 1976; Hurst 1975; Dorning & Bell 1987; Corfield *et al.* 1992; Ratcliffe & Thomas 1999). This is largely due to the lateral facies variations between the two areas, their positions on the Midland Platform, and the relatively limited biostratigraphical control provided by graptolites. Detailed local correlation of the formation across the Midland Platform now involves integrated studies of sequence stratigraphy (Ray & Thomas 2007, Ray & Butcher 2010, Ray *et al.* 2010), bentonite geochemical fingerprinting (Ray *et al.* 2011) and biostratigraphy, as summarized below (see Ray *et al.* 2010 for further details).

The Much Wenlock Limestone Formation of the West Midlands consists of two shallow water limestones (Lower Quarried Limestone and Upper Quarried Limestone members), separated by a deeper water nodular limestone and silty mudstone-rich interval (Nodular Beds Member). On the basis of specimens of *Monograptus flemingii* collected 2.4 m above the base of the Lower Quarried Limestone Member (Butler 1939), an age no younger than the *lundgreni* Biozone has been inferred (Bassett 1974) for that part of the sequence. No precisely located graptolites have been recovered from the remainder of the formation or the overlying Lower Elton Formation. However, graptolite specimens that are presumed to have originated from the exposed basal 13.2 m of the Lower Elton Formation at Dudley suggest a *Neodiversograptus nilssoni* to *Lobograptus scanicus* biozone age (Bassett 1976). It therefore seems likely that the Much Wenlock Limestone Formation of the West Midlands spans the upper *lundgreni* through to *ludensis* biozones.

On Wenlock Edge a sequence spanning the *lundgreni* to *nilssoni* biozones is represented in the uppermost Apedale Member and Farley Member (Coalbrookdale Formation), Much Wenlock Limestone Formation and basal Lower Elton Formation. The Wenlock Series in the type area yields age-diagnostic graptolites; however, these are restricted to a small number of key sections within the off-reef tract (a shelf–basin-margin setting developed below the water depth required for reef growth; see Bassett 1989). Although these sections are approximately 10 to 15 km southwest of those sampled here, correlations based on sequence stratigraphy and lithostratigraphy can be made (Ray & Butcher 2010, Ray *et al.* 2010). The Lower Hill Farm Track is the stratigraphically oldest of the sections sampled and exposes 21 m of the uppermost Apedale Member. The contact with the overlying Farley Member cannot be seen; however, it is estimated to occur 5 to 25 m above the top of the section (Dorning & Harvey 1999, Ray & Butcher 2010).

Within the off-reef tract the Eaton Track section contains the stratotype for the base of the (upper) Gleedon Chronozone of the Homerian Stage (Bassett *et al.* 1975) and the Apedale/Farley Member boundary. There the LAD of *Monograptus flemingii* marks the *lundgreni/nassa* biozone boundary and occurs 9.5 m below the first limestone bands that mark the base of the Farley Member. Based upon an approximate synchronicity of the Apedale/Farley Member boundary along Wenlock Edge, the *lundgreni* Biozone should therefore occupy at the very least the majority of the Lower Hill Farm Track section, and according to Ray *et al*. (2010) the upper boundary of the *lundgreni* Biozone may well occur in the overlying basal Farley Member.

The boundary between the Farley Member and the Much Wenlock Limestone Formation is diachronous along Wenlock Edge, with the base of the Much Wenlock Limestone Formation being slightly older (three additional parasequences) within the reef tract (a shelf–basin-margin setting where reef development is common) succession (Ray *et al.* 2010). The boundary between the Farley Member and the Much Wenlock Limestone Formation in the off-reef tract is exposed in the Longville–Stanway road cutting (Ray *et al.* 2010). *Monograptus ludensis* and *Pristiograptus jaegeri* recorded from 0.9 m below the top of the Farley Member, and *M. ludensis* and other graptolites from 0.6, 3.9 and 5.7 m above the base of the Much Wenlock Limestone Formation, indicate that the formation's lower boundary lies within the *ludensis* Biozone (Bassett *et al.* 1975) within the off-reef tract and potentially within the *nassa* Biozone within the reef tract. Age-diagnostic graptolites have not been collected from the upper part of the Much Wenlock Limestone Formation; however, the geochemical fingerprinting and correlation of a bentonite along Wenlock Edge and eastwards to Dudley (Ray *et al.* 2011) argues for synchronicity. The Lower Elton Formation along Wenlock Edge also contains age-diagnostic graptolites: *Monograptus uncinatus orbatus* (White 1974) and *Colonograptus colonus* (Loydell & Fone 1998) indicate that the basal Lower Elton Formation is at or near the base of the lowest Ludlow *nilssoni* Biozone, as is the case for the West Midlands.

A sequence stratigraphical interpretation consistent with the available biostratigraphical data forms the basis for the correlation shown in Fig. 2. Ray & Thomas (2007) established a framework for the Much Wenlock Limestone Formation in the West Midlands, identifying thirteen parasequences between the base of the unit and the lowest part of the Lower Elton Formation. Although differences do exist – due to differences in water depth and position relative to the platform margin – the same number of parasequences can be recognised on Wenlock Edge (Ray *et al*. 2010). While lithofacies patterns suggest that some degree of westerly younging remains likely at the top of the formation, it must have been less than Bassett (1974) and Ratcliffe & Thomas (1999) considered it to be; that is the degree of diachronism cannot be greater than the time taken to have deposited Parasequence 11 (Ray *et al*. 2010). The variations in carbon isotope ratios found in our samples are initially discussed on the assumption that this stratigraphical framework is correct, with alternative possibilities discussed subsequently.

## Results

The carbon isotope results are summarized in Fig. 2. Although differences between the two data sets are apparent, they feature one or two large positive carbon isotope peaks with smaller-scale, shorter-term variations superimposed. In the West Midlands composite section, $\delta^{13}$C values rise from near zero at the top of the Coalbrookdale Formation to +5.5‰ VPDB in the Lower Quarried Limestone Member (lower part of *nassa* Biozone; Ray *et al.* 2010). Near the base of the Nodular Beds Member (higher part of *nassa* Biozone) values fall to +0.8‰ VPDB. A second stratigraphically longer positive peak then occurs in the upper part of the Nodular Beds Member (*ludensis* Biozone) with $\delta^{13}$C values rising to +4.1‰ VPDB. Overall values then decline through the upper part of the Nodular Beds Member and Upper Quarried Limestone, averaging +0.3‰ VPDB in the overlying Lower Elton Formation, near the Wenlock/Ludlow boundary. The two positive peaks in this section are punctuated by a number of short-lived negative events in which $\delta^{13}$C values fall to –0.1‰VPDB. Although not shown (see Appendices) $\delta^{18}$O also fall sharply during these times; however, in other parts of the section $\delta^{13}$C and $\delta^{18}$O values are not strongly correlated.

In the lower part of the succession from Wenlock Edge, the uppermost Apedale and Farley members (of the Coalbrookdale Formation) have relatively constant $\delta^{13}$C values around +2.0‰VPDB. Higher in the Much Wenlock Limestone Formation, values do rise to +3.8‰ VPDB and, although less distinct, this corresponds with the younger positive peak found in the West Midlands. In both sections, the base of this positive excursion event lies within

Parasequence 9 and its peak occurs within Parasequence 10 (Ray & Thomas 2007, Ray *et al.* 2010; see Fig. 2). However, above this and towards the top of the Much Wenlock Limestone Formation, the curves and absolute isotopic values differ. The West Midlands section shows a relatively rapid decline from a +3.9‰ VPDB peak low in Parasequence 10 to +0.3‰ VPDB in the middle of Parasequence 11, below the Lower Elton–Much Wenlock Limestone Formation boundary. Above this, values are near constant around +0.6‰ VPDB. A more gradual decline in $\delta^{13}C$ values occurs on Wenlock Edge, with values of +3.8‰ VPDB in Parasequence 10, +2.5‰ VPDB at the Lower Elton–Much Wenlock Limestone Formation boundary (top of Parasequence 11), above which values decline to ~ +1.0‰ VPDB within Parasequence 14.

## Discussion and comparisons

The section sampled in the West Midlands covers a somewhat thicker stratigraphical interval than that documented previously (Corfield *et al.* 1992). The overall double-peaked $\delta^{13}C$ curve obtained from the West Midlands is generally similar. Our $\delta^{13}C$ values are consistently some +2‰ VPDB heavier, although Corfield *et al.* (1992) did not state the standards used in their analyses. Although differences between the Wenlock Edge and West Midlands sections are apparent, our values generally correspond better with those obtained elsewhere, that is peak $\delta^{13}C$ values of +4.6‰ from the East Baltic (Kaljo *et al.* 1997), 3.8‰ from Gotland (Calner *et al.* 2006), +2.5‰ from Nevada (Cramer *et al.* 2006) and +2.8‰ from Tennessee (Cramer *et al.* 2006); for review, see Calner (2008).

Both sections feature one or two large positive carbon isotope peaks with smaller-scale, shorter-term variations superimposed. This Homerian positive excursion (Mulde) is one of three that have been recognised widely in Llandovery and Wenlock rocks (Saltzman 2001, Calner 2008). In arctic Canada and Gotland (Loydell 2007), the excursion is double-peaked, and the two peaks appear approximately synchronous with those in the English Midlands, within the limits of biostratigraphical resolution. A double peak has been identified in the Homerian of Podolia (Ukraine) too, however both peaks occur in the *ludensis* Biozone there (Kaljo *et al.* 2007). Kaljo *et al.* (1997) identified a single excursion in the *nassa* Biozone of the East Baltic. To what extent some of these regional differences are real, perhaps reflecting variations in geological setting relative to the local basin margin, as opposed to uncertainties in detailed correlation or matters relating to sampling, remains to be established. Further understanding of these issues will enhance the value of the isotopic variations for increasing confidence in international correlation at the stage level and below. This would be particularly valuable in sections that are barren of graptolites and/or conodonts, and between sections that contain these fossils and others that do not.

Given that variations in $\delta^{13}C_{carb}$ ratios ultimately reflects carbon cycling in the oceans, it is surprising that some significant contrasts should exist between two composite sections separated by only approximately 40 km. An alternative possibility is that our understanding of the correlation of the Much Wenlock Limestone Formation in the area requires significant revision. Correlation along Wenlock Edge between the reef tract (study area) and the graptolite-bearing off-reef tract, indicates that the base of the Farley Member (Coalbrookdale Formation) corresponds approximately to the top of the *lundgreni* Biozone, correlating with the base of the Lower Quarried Limestone Member (Much Wenlock Limestone Formation) in the West Midlands (see Ray *et al*. 2010). Based on comparison between the parasequences of Ray & Thomas (2007) and the carbon isotopic values for the West Midlands, Parasequences 3 to 7 correspond to the low values found within the Mulde Excursion. This interval (Parasequences 3 to 7) represents a relatively condensed interval on Wenlock Edge (Ray *et al*. 2010) and has consequently been sampled at ~20 cm intervals in order to attempt to identify these reduced values. At present no such low in values can be recognised on Wenlock Edge. Throughout the uppermost Apedale, Farley Member and lower Much Wenlock Limestone Formation, $\delta^{13}C$ values remain relatively constant at around +2.0‰ VPDB. A possible explanation for the apparent lack of the lower positive event on Wenlock Edge would be that the interval of ~2‰ VPDB values recorded there is actually an extended record of the low-point between the two positive peaks found in the West Midlands. This would not only be completely inconsistent with the sequence stratigraphy however, but also with the biostratigraphy: the lower peak on Wenlock Edge would then have to occur below the part of the section sampled, and lie within the *lundgreni* Biozone rather than in the *nassa* Biozone.

Correlation of the upper Mulde peak shows that maximum $\delta^{13}C$ values correspond to the middle of Parasequence 10 (Ray *et al.* 2010) at both locations; an interval additionally constrained by the correlation of bentonites (Ray *et al.* 2011). Absolute $\delta^{13}C$ values are also very similar, +3.8‰ and +3.9 VPDB‰ at Wenlock Edge and Dudley respectively. However the decline in values is relatively rapid in the West Midlands with the declining limb being contained within the upper Much Wenlock Limestone Formation (Parasequence 10 and Parasequence 11). A similar pattern is recorded at the platform margin, Pitch Coppice (Ludlow) and within a mid-platform location at Gurney's Quarry (Malvern Hills) (Corfield *et al.* 1992). The decline from peak $\delta^{13}C$ values on Wenlock Edge ap-

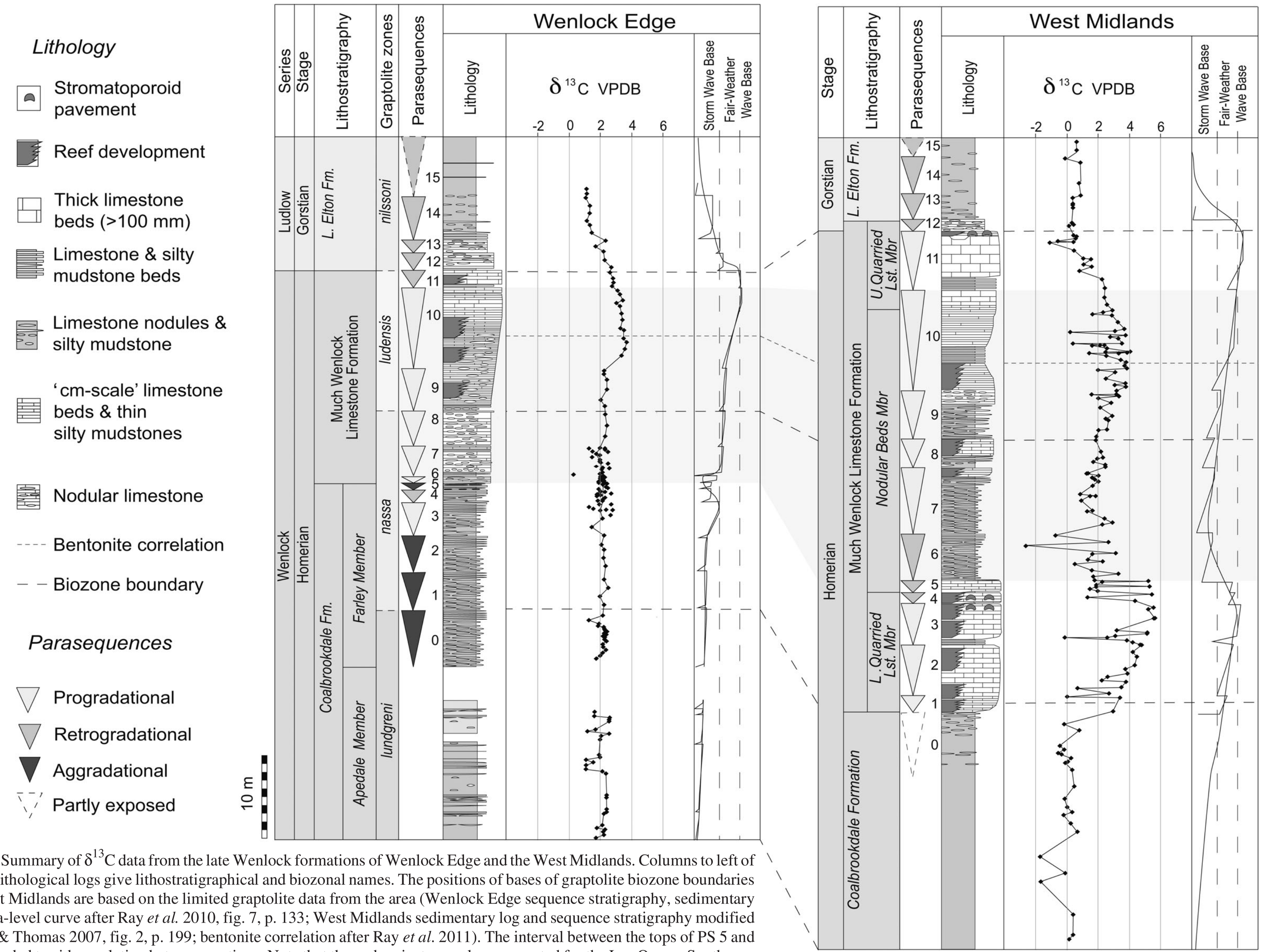


**Figure 2.** Summary of $\delta^{13}C$ data from the late Wenlock formations of Wenlock Edge and the West Midlands. Columns to left of summary lithological logs give lithostratigraphical and biozonal names. The positions of bases of graptolite biozone boundaries in the West Midlands are based on the limited graptolite data from the area (Wenlock Edge sequence stratigraphy, sedimentary log and sea-level curve after Ray *et al.* 2010, fig. 7, p. 133; West Midlands sedimentary log and sequence stratigraphy modified from Ray & Thomas 2007, fig. 2, p. 199; bentonite correlation after Ray *et al.* 2011). The interval between the tops of PS 5 and PS 10 is shaded to aid correlation between sections. Note that the carbon isotope values presented for the Lea Quarry South section in Thomas *et al.* (2011, fig. 37) were plotted some 5 m too high stratigraphically, due to a drafting error.

pears more gradual than in the West Midlands section, with elevated values observed some 6 m into the Lower Elton Formation. This is unusual when compared with other Midland Platform sections from a variety of depositional settings and may reflect the local response of the carbonate system to transgression towards the end of Wenlock time. In all sections, excluding an area known as Hill Top (an area where reefs are most abundant within the reef tract) on Wenlock Edge, the onset of transgression (Parasequence 11) is marked by a basinal shift in facies with only local grainstone shoals (such as at Wren's Nest Hill, Dudley) and occasional small reefs developed. Above Parasequence 11, limestones are much less common and silty-mudstones dominate, marking the drowning of the carbonate system. However, around Hill Top, Wenlock Edge (Lea South Quarry sample area) the barrier-like reef complex continued to keep up with sea-level rise within Parasequence 11, remaining a sea-floor high until at least Parasequence 13, as evidenced by the development of nodular limestones (Ray *et al.* 2010). The anomalous decline in $\delta^{13}C$ values at Wenlock Edge could therefore be associated with the shallowest marine facies developed on the Midland Platform at that time, or reflect processes taking place close to the shelf-basin margin, such as upwelling.

The top of the upper excursion in the West Midlands lies in the middle of Parasequence 11, within the Upper Quarried Limestone Member, whereas on Wenlock Edge the upper excursion extends into Parasequence 13, well within the Lower Elton Formation. The carbon isotope data thus suggest diachronism at the base of the Lower Elton Formation, whose base would have to be significantly older on Wenlock Edge, not younger as some authors have argued previously. Again this possibility is inconsistent not only with the sequence stratigraphical framework and regional lithofacies patterns, but also with biostratigraphy. Although graptolite data from the lower part of the Lower Elton Formation are limited, its basal boundary on Wenlock Edge lies at or very close to the base of the *nilssoni* Biozone (Bassett 1989). Only 13.2 m of the Lower Elton Formation are exposed in the Wren's Nest Inlier of the West Midlands. *Saetograptus* and *Monograptus* species are recorded from this interval (Bassett 1976, Siveter *in* Aldridge *et al.* 2000), including *S. chimaera*, which does not occur below the *nilssoni* Biozone. These biostratigraphical data preclude diachronism of the extent required.

## Acknowledgements

We thank Axel Munnecke, Pat McLaughlin and an anonymous referee for their constructively critical comments on an earlier version of the manuscript. We thank also Dudley Museum and Bardon Aggregates for access to sections. West Midlands sedimentary log and sequence stratigraphy are after Ray & Thomas (2007), reproduced with the permission of the Palaeontological Association. Wenlock Edge sequence stratigraphy, sedimentary log and sea-level curve after Ray *et al.* (2010) from the *Geological Magazine* are reproduced with the permission of Cambridge University Press.

## References

ALDRIDGE, R.J., SIVETER, DAVID J., SIVETER, DEREK, J., LANE, P.D., PALMER, D.C. & WOODCOCK, N.H. 2000. *British Silurian stratigraphy*. xvii + 542 pp. Geological Conservation Review Series, Joint Nature Conservation Committee, Peterborough.

BASSETT, M.G. 1974. Review of the stratigraphy of the Wenlock Series in the Welsh Borderland and South Wales. *Palaeontology 17*, 145–177.

BASSETT, M.G. 1976. A critique of diachronism, community distribution and correlation of the Wenlock–Ludlow boundary. *Lethaia 9*, 201–218.

BASSETT, M.G. 1989. The Wenlock Series in the Wenlock area, 51–73. *In* BASSETT, M.G. & HOLLAND, C.H. (eds) *A global standard for the Silurian System. National Museum of Wales, Geological Series 9*.

BASSETT, M.G., COCKS, L.R.M., HOLLAND, C.H., RICKARDS, R.B. & WARREN, P.T. 1975. The type Wenlock Series. *Institute of Geological Sciences Report 75/13*, 1–19.

BUTLER, A.J. 1939. The stratigraphy of the Wenlock Limestone at Dudley. *Quarterly Journal of the Geological Society of London 95*, 34–74. DOI 10.1144/GSL.JGS.1939.065.01-04.04

CALNER, M. 2008. Silurian global events – at the tipping point of climate change, 21–57. *In* ELEWA, A.M.T. (ed.) *Mass extinctions*. Springer, Berlin & Heidelberg. DOI 10.1007/978-3-540-75916-4_4

CALNER, M., KOZŁOWSKA, A., MASIAK, M. & SCHMITZ, B. 2006. A shoreline to deep basin correlation chart for the middle Silurian coupled extinction-stable isotopic event. *GFF 128*, 79–84. DOI 10.1080/11035890601282079

CORFIELD, R.M., SIVETER, DEREK, J., CARTLIDGE, J.E. & MCKERROW, W.S. 1992. Carbon isotope excursions near the Wenlock–Ludlow (Silurian) boundary in the Anglo-Welsh area. *Geology 20*, 371–374. DOI 10.1130/0091-7613(1992)020<0371:CIENTW>2.3.CO;2

CRAMER, B.D., KLEFFNER, M.A. & SALTZMAN, M.R. 2006. The Late Wenlock Mulde positive carbon isotope ($\delta^{13}C_{carb}$) excursion in North America. *GFF 128*, 85–90. DOI 10.1080/11035890601282085

DORNING, K.J. & BELL, D.G. 1987. The Silurian shelf microfacies: acritarch distribution in the Much Wenlock Limestone Formation, 266–287. *In* HART, M.B. (ed.) *Micropalaeontology of carbonate environments*. Ellis Horwood, Chichester.

DORNING, K.J. & HARVEY, C. 1999. Wenlock cyclicity, palynology, and stratigraphy in the Buildwas, Coalbrookdale, and Much Wenlock Limestone formations, Shropshire, England. *Bollettino della Società Paleontologica Italiana 38*, 155–166.

GRAHN, Y. & CAPUTO, M.V. 1992. Early Silurian glaciations in Brazil. *Palaeogeography, Palaeoclimatology, Palaeoecology 99*, 9–15. DOI 10.1016/0031-0182(92)90003-N

Hurst, J.M. 1975. The diachronism of the Wenlock Limestone. *Lethaia 8*, 301–314. DOI 10.1111/j.1502-3931.1975.tb00935.x

Johnson, M.A. 2006. Relationship of Silurian sea-level fluctuations to oceanic episodes and events. *GFF 128*, 115–121. DOI 10.1080/11035890601282115

Kaljo, D., Grytsenko, V., Martma, T. & Mõtus, M.-A. 2007. Three global carbon isotope shifts in the Silurian of Podolia (Ukraine): stratigraphical implications. *Estonian Journal of Earth Sciences 56*, 205–220. DOI 10.3176/earth.2007.02

Kaljo, D., Kiipli, T. & Martma, T. 1997. Carbon isotope event markers through the Wenlock–Přídolí sequence at Ohesaare (Estonia) and Priekule (Latvia). *Palaeogeography, Palaeoclimatology, Palaeoecology 132*, 211–223. DOI 10.1016/S0031-0182(97)00065-5

Loydell, D.K. 2007. Early Silurian positive $\delta^{13}C$ excursions and their relationship to glaciations, sea-level changes and extinction events. *Geological Journal 42*, 531–546. DOI 10.1002/gj.1090

Loydell, D.K. & Fone, W. 1998. Graptolites from the Lower Elton Formation (Ludlow) of Shadwell Rock Quarry, Shropshire. *Geological Journal 33*, 147–148. DOI 10.1002/(SICI)1099-1034(199807/09)33:3<147::AID-GJ785>3.0.CO;2-W

Melchin, M.J. & Holmden, C. 2006. Carbon isotope chemostratigraphy of the Llandovery in Arctic Canada: implications for global correlation and sea level change. *GFF 128*, 173–180. DOI 10.1080/11035890601282173

Munnecke, A., Calner, M., Harper, D.A.T. & Servais, T. 2010. Ordovician and Silurian sea-water chemistry, sea level, and climate: a synopsis. *Palaeogeography, Palaeoclimatology, Palaeoecology 296*, 389–413. DOI 10.1016/j.palaeo.2010.08.001

Ratcliffe, K.T. 1991. Palaeoecology, taphonomy and distribution of brachiopod assemblages from the Much Wenlock Limestone Formation of England and Wales. *Palaeogeography, Palaeoclimatology, Palaeoecology 83*, 265–293. DOI 10.1016/0031-0182(91)90056-W

Ratcliffe, K.T. 1999. Brachiopod assemblages from the Much Wenlock Limestone Formation of England and Wales, 592–637. *In* Boucot, A.J. & Lawson, J.D. (eds) *Paleocommunities – a case study from the Silurian and Lower Devonian*. Cambridge University Press, Cambridge.

Ratcliffe, K.T. & Thomas, A.T. 1999. Carbonate depositional environments in the late Wenlock of England and Wales. *Geological Magazine 136*, 189–204. DOI 10.1017/S0016756899002538

Ray, D.C. 2007. The correlation of lower Wenlock Series (Silurian) bentonites from the Lower Hill Farm and Eastnor Park boreholes, Midland Platform, England. *Proceedings of the Geologists' Association 118*, 175–185.

Ray, D.C., Brett, C.E., Thomas, A.T. & Collings, A.V.J. 2010. Late Wenlock sequence stratigraphy in central England. *Geological Magazine 147*, 123–144. DOI 10.1017/S0016756809990197

Ray, D.C., Collings, A.V.J., Worton, G.J. & Jones, G. 2011. Upper Wenlock bentonites from Wren's nest Hill, Dudley: comparisions with prominent bentonites along Wenlock Edge, Shropshire, England. *Geological Magazine 148*, 670–681. DOI 10.1017/S0016756811000288

Ray, D.C. & Butcher, A. 2010. Sequence stratigraphy of the type Wenlock area (Silurian), England. *Bollettino della Società Paleontologica Italiana 49*, 47–54.

Ray, D.C. & Thomas, A.T. 2007. Carbonate depositional environments, sequence stratigraphy and exceptional skeletal preservation in the Much Wenlock Limestone Formation (Silurian) of Dudley, England. *Palaeontology 50*, 197–222. DOI 10.1111/j.1475-4983.2006.00607.x

Saltzmann, M.R. 2001. Silurian $\delta^{13}C$ stratigraphy: a view from North America. *Geology 29*, 671–674. DOI 10.1130/0091-7613(2001)029<0671:SCSAVF>2.0.CO;2

Scoffin, T.P. 1971. The conditions of growth of the Wenlock reefs of Shropshire. *Sedimentology 17*, 173–219. DOI 10.1111/j.1365-3091.1971.tb01774.x

Thomas, A.T. 1978. British Wenlock trilobites. Part 1. *Monograph of the Palaeontographical Society 132(552)*, 1–56.

Thomas, A.T., Marshall, C. & Ray, D.C. 2011. Reef and inter-reef facies in the Much Wenlock Limestone Formation and overlying Lower Elton Formation, Lea Quarry South, Wenlock Edge, 114–121. *In* Ray, R.C. (ed.) *Siluria revisited: a field guide. International Subcommission on Silurian Stratigraphy, Field Meeting 2011*. 170 pp. MPG Books, Bodmin.

White, D.E. 1974. The boundary between the Wenlock and Ludlow Series. *Geological Magazine 111*, 448–449. DOI 10.1017/S0016756800040048

## Appendix 1

$\delta^{13}C_{carb}$ and $\delta^{18}O$ data from the West Midlands and Wenlock Edge. Key to locality codes as follows:
West Midlands – WN1. WN2: Wrens Nest (SO 938 921). MHC. 2C: Mons Hill Core (SO 938 923). SS: Step Shaft Mine (SO 939 918).

| Lab Code | Locality Code | Depth on composite section | $\delta^{13}C$ | $\delta^{18}O$ |
|---|---|---|---|---|
| CLY198 | SS3 | –0.5 | 0.58 | –6.37 |
| CLY199 | SS3 | –1.5 | 0.62 | –5.85 |
| CLY200 | SS3 | –2.5 | –0.13 | –6.49 |
| CLY201 | SS3 | –3.0 | 0.84 | –7.02 |
| CLY202 | SS3 | –5.3 | 0.87 | –7.31 |
| CLY203 | SS3 | –5.5 | 0.77 | –6.15 |
| CLY204 | SS3 | –7.0 | 0.89 | –7.26 |
| CLY205 | SS3 | –7.3 | 0.36 | –7.27 |
| CLY206 | SS3 | –8.0 | 0.38 | –8.26 |
| CRLY169 | SS1 | –8.1 | 0.36 | –6.19 |
| CLY207 | SS3 | –8.5 | 0.39 | –5.47 |
| CRLY170 | SS2 | –10.3 | 0.30 | –6.15 |
| CLY208 | SS3 | –10.5 | 0.42 | –6.20 |
| CRLY171 | SS3 | –10.6 | 0.12 | –6.27 |
| CRLY172 | SS4 | –11.6 | 0.38 | –6.88 |
| CLY134 | 2C1 | –11.8 | 0.42 | –5.80 |
| CLY009 | MHC1 | –12.0 | 0.61 | –6.17 |
| CLY135 | 2C2 | –12.2 | 0.55 | –5.22 |
| CLY136 | 2C3 | –12.5 | –0.62 | –7.95 |
| CRLY173 | SS5 | –12.6 | 0.41 | –6.53 |
| CLY010 | MHC2 | –12.7 | –1.13 | –8.42 |
| CRLY174 | SS6 | –13.6 | 0.43 | –7.93 |
| CRLY175 | SS7 | –14.6 | 1.02 | –5.11 |
| CRLY176 | SS8 | –14.7 | 1.55 | –7.04 |
| CLY011 | MHC3 | –15.3 | 1.03 | –7.99 |
| CLY137 | 2C4 | –15.6 | 1.61 | –6.10 |
| CRLY177 | SS9 | –16.1 | 0.79 | –12.68 |
| CRLY178 | SS10 | –17.1 | 2.23 | –8.48 |
| CRLY179 | SS11 | –18.2 | 2.40 | –8.51 |
| CRLY180 | SS12 | –19.3 | 2.36 | –7.52 |
| CRLY181 | SS13 | –20.2 | 2.54 | –6.58 |
| CLY012 | MHC4 | –20.9 | 2.90 | –7.19 |
| CRLY182 | SS14 | –21.1 | 2.28 | –8.19 |
| CRLY183 | SS15 | –21.4 | 1.61 | –6.31 |
| CLY013 | MHC5 | –21.5 | 2.85 | –6.34 |
| CLY014 | MHC6 | –22.3 | 3.22 | –5.93 |
| CLY015 | MHC7 | –23.1 | 3.65 | –5.56 |
| CRLY184 | SS16 | –23.4 | 3.02 | –5.87 |
| CLY001 | WN1 C1 | –23.5 | 0.17 | –7.63 |
| CLY016 | MHC8 | –23.9 | 3.72 | –6.00 |
| CRLY185a | SS17 | –24.1 | 2.68 | –6.21 |
| CLY017 | MHC9 | –24.3 | 3.25 | –5.44 |

| Lab Code | Locality Code | Depth on composite section | $\delta^{13}C$ | $\delta^{18}O$ |
|---|---|---|---|---|
| CLY018 | MHC10 | –24.9 | 3.50 | –5.49 |
| CLY005 | WN1 C6 | –24.9 | 0.35 | –8.72 |
| CLY002 | WN1 C3 | –25.1 | 2.08 | –6.28 |
| CRLY186 | SS18 | –25.1 | 2.36 | –6.98 |
| CLY003 | WN1 C4 | –25.1 | 1.55 | –6.76 |
| CLY004 | WN1 C5 | –25.4 | 2.51 | –6.28 |
| CLY019 | MHC11 | –25.9 | 3.99 | –5.56 |
| CLY006 | WN1 C7 | –25.9 | 2.42 | –6.61 |
| CLY020 | MHC12 | –26.0 | 3.83 | –5.01 |
| CLY007 | WN1 C8 | –26.1 | 1.41 | –5.83 |
| CRLY187 | SS19 | –26.1 | 3.27 | –6.39 |
| CLY008 | WN1 C9 | –26.3 | 2.47 | –7.95 |
| CLY021 | MHC13 | –26.9 | 3.38 | –6.36 |
| CRLY188 | SS20 | –27.1 | 3.74 | –5.63 |
| CRLY189 | SS21 | –27.6 | 3.63 | –6.55 |
| CLY022 | MHC14 | –27.9 | 3.78 | –4.84 |
| CRLY190 | SS22 | –28.1 | 1.93 | –7.59 |
| CLY023 | MHC15 | –28.3 | 3.06 | –6.74 |
| CLY024 | MHC16 | –29.1 | 2.43 | –6.14 |
| CRLY191 | SS23 | –29.7 | 3.69 | –5.65 |
| CLY025 | MHC17 | –29.9 | 2.99 | –5.39 |
| CRLY192 | SS24 | –30.1 | 3.76 | –5.76 |
| CRLY193 | SS25 | –30.6 | 3.13 | –5.81 |
| CLY026 | MHC18 | –31.0 | 3.12 | –5.78 |
| CRLY194 | SS26 | –31.1 | 1.54 | –8.35 |
| CLY027 | MHC19 | –31.3 | 3.28 | –5.72 |
| CLY028 | MHC20 | –31.5 | 1.95 | –7.17 |
| CRLY195 | SS27 | –32.1 | 2.79 | –5.59 |
| CLY029 | MHC21 | –32.7 | 2.08 | –8.31 |
| CLY030 | MHC22 | –33.6 | 2.89 | –4.80 |
| CLY031 | MHC23 | –34.0 | 2.45 | –5.70 |
| CLY032 | MHC24 | –34.2 | 2.63 | –6.09 |
| CLY033 | MHC25 | –35.3 | 2.53 | –5.18 |
| CRLY196 | SS28 | –35.4 | 2.02 | –5.13 |
| CLY034 | MHC26 | –36.2 | 1.87 | –6.80 |
| CRLY197 | SS29 | –36.6 | 1.82 | –5.37 |
| CRLY198 | SS30 | –38.0 | 2.13 | –5.80 |
| CLY035 | MHC28 | –38.7 | 2.27 | –5.26 |
| CLY249 | SS3 | –38.9 | 1.92 | –8.10 |
| CLY036 | MHC29 | –39.2 | 1.66 | –5.71 |
| CLY037 | MHC30 | –39.6 | 2.43 | –5.86 |
| CLY248 | SS3 | –39.9 | 2.44 | –5.25 |

| Lab Code | Locality Code | Depth on composite section | $\delta^{13}C$ | $\delta^{18}O$ |
|---|---|---|---|---|
| CLY247 | SS3 | –40.6 | 1.32 | –6.27 |
| CLY038 | MHC31 | –40.6 | 1.23 | –7.51 |
| CLY246 | SS3 | –40.9 | 2.00 | –6.92 |
| CLY245 | SS3 | –41.1 | 1.59 | –8.34 |
| CLY244 | SS3 | –41.4 | 1.75 | –8.02 |
| CLY243 | SS3 | –41.6 | 2.00 | –6.93 |
| CLY242 | SS3 | –42.1 | 1.60 | –9.25 |
| CLY039 | MHC32 | –43.1 | 0.83 | –5.59 |
| CLY241 | SS3 | –43.4 | 1.45 | –9.22 |
| CLY240 | SS3 | –43.4 | 1.80 | –7.71 |
| CLY040a | MHC33 | –43.9 | 0.90 | –6.03 |
| CLY239 | SS3 | –45.1 | 1.64 | –5.30 |
| CLY041 | MHC34 | –45.2 | 1.27 | –7.55 |
| CLY238 | SS3 | –46.1 | 2.37 | –6.28 |
| CLY237 | SS3 | –46.6 | 2.86 | –4.81 |
| CLY042 | MHC35 | –46.8 | 2.23 | –8.15 |
| CLY236 | SS3 | –48.1 | –0.76 | –8.53 |
| CLY043 | MHC36 | –49.0 | 2.61 | –6.64 |
| CLY235 | SS3 | –49.4 | –2.62 | –8.21 |
| CLY044 | MHC37 | –50.3 | 3.07 | –5.51 |
| CLY234 | SS3 | –50.4 | 1.60 | –7.95 |
| CLY233 | SS3 | –51.1 | 1.33 | –9.04 |
| CLY045 | MHC38 | –51.3 | 2.26 | –7.87 |
| CLY232 | SS3 | –51.6 | 0.50 | –5.32 |
| CLY231 | SS3 | –52.4 | 1.56 | –8.47 |
| CLY046 | MHC39 | –52.8 | 3.23 | –8.51 |
| CLY230 | SS3 | –53.1 | 1.65 | –5.02 |
| CLY229 | SS3 | –53.6 | 1.75 | –8.55 |
| CLY067 | WN2 C15 | –53.7 | 5.15 | –6.07 |
| CLY047 | MHC40 | –53.8 | 2.22 | –8.00 |
| CLY228 | SS3 | –54.1 | 1.84 | –7.56 |
| CLY068 | WN2 C14 | –54.3 | 5.20 | –6.19 |
| CLY227 | SS3 | –54.4 | 1.84 | –7.85 |
| CLY226 | SS3 | –54.6 | 1.44 | –9.05 |
| CLY225 | SS3 | –54.9 | 1.94 | –8.98 |
| CLY069 | WN2 C13 | –55.2 | 5.36 | –6.42 |
| CLY224 | SS3 | –55.6 | 1.28 | –8.36 |
| CLY048 | MHC43 | –56.0 | 4.30 | –7.18 |
| CLY070 | WN2 C12 | –56.8 | 5.48 | –6.36 |
| CLY049 | MHC44 | –57.0 | 5.11 | –6.70 |
| CLY050 | MHC45 | –58.1 | 5.52 | –6.16 |
| CLY138 | 2C5 | –58.1 | 5.54 | –5.26 |
| CLY071 | WN2 C11 | –59.6 | 3.15 | –5.19 |
| CLY139 | 2C6 | –59.9 | 5.06 | –6.25 |
| CLY140 | 2C7 | –60.0 | 5.05 | –6.33 |

| Lab Code | Locality Code | Depth on composite section | $\delta^{13}C$ | $\delta^{18}O$ |
|---|---|---|---|---|
| CLY141 | 2C8 | –60.3 | 3.04 | –7.30 |
| CLY051 | MHC46 | –60.5 | –0.14 | –8.95 |
| CLY142 | 2C9 | –60.5 | 2.53 | –7.29 |
| CLY143 | 2C10 | –60.8 | 3.77 | –6.39 |
| CLY144 | 2C11 | –61.1 | 4.15 | –6.82 |
| CLY052 | MHC47 | –61.3 | 4.61 | –5.47 |
| CLY145 | 2C12 | –61.3 | 4.63 | –5.21 |
| CLY072 | WN2 C10 | –61.4 | 4.72 | –6.84 |
| CLY073 | WN2 C9 | –62.2 | 4.15 | –8.23 |
| CLY053 | MHC49 | –62.8 | 4.42 | –6.57 |
| CLY074 | WN2 C8 | –63.8 | 4.27 | –6.44 |
| CLY054 | MHC50 | –64.3 | 3.67 | –6.75 |
| CLY075 | WN2 C7 | –64.8 | 3.83 | –7.76 |
| CLY055 | MHC51 | –65.2 | 2.57 | –5.77 |
| CLY056 | MHC54 | –65.7 | 2.20 | –5.78 |
| CLY076 | WN2 C6 | –65.8 | 3.73 | –5.83 |
| CLY077 | WN2 C5 | –66.5 | 3.43 | –7.72 |
| CLY057 | MHC55 | –66.6 | 0.66 | –7.14 |
| CLY078 | WN2 C4 | –67.2 | 2.64 | –9.53 |
| CLY058 | MHC56 | –67.7 | 0.01 | –5.52 |
| CLY079 | WN2 C3 | –67.8 | 3.32 | –5.69 |
| CLY081 | WN2 C1 | –69.4 | 2.89 | –4.85 |
| CLY059 | MHC60 | –71.0 | –0.17 | –8.08 |
| CLY060 | MHC61 | –71.7 | 0.77 | –6.37 |
| CLY061 | MHC62 | –73.6 | –0.45 | –6.51 |
| CLY062 | MHC64 | –74.1 | –0.19 | –6.46 |
| CLY063 | MHC65 | –74.5 | –0.56 | –6.44 |
| CLY064 | MHC66 | –74.7 | –0.35 | –7.06 |
| CLY065 | MHC67 | –75.1 | 0.24 | –7.69 |
| CLY209 | SS3 | –75.5 | 0.04 | –8.27 |
| CLY066 | MHC68 | –75.6 | –0.10 | –7.59 |
| CLY210 | SS3 | –76.5 | 0.33 | –7.21 |
| CLY211 | SS3 | –78.5 | 0.45 | –6.19 |
| CLY212 | SS3 | –80.0 | –0.15 | –6.69 |
| CLY213 | SS3 | –81.0 | 0.02 | –7.35 |
| CLY214 | SS3 | –81.6 | 0.32 | –6.75 |
| CLY215 | SS3 | –82.0 | –0.21 | –6.30 |
| CLY216 | SS3 | –83.0 | 0.22 | –8.32 |
| CLY217 | SS3 | –84.0 | 0.65 | –6.36 |
| CLY218 | SS3 | –87.0 | –1.69 | –6.09 |
| CLY219 | SS3 | –89.0 | –0.10 | –6.84 |
| CLY220 | SS3 | –90.0 | –1.66 | –6.86 |
| CLY221 | SS3 | –94.0 | 0.39 | –6.23 |
| CLY222 | SS3 | –96.5 | 0.37 | –6.86 |
| CLY223 | SS3 | –97.0 | 0.12 | –6.26 |

## Appendix 2

Wenlock Edge – LQ: Lea Quarry South (SO 594 982). HH: Harley Hill (SJ 609 004). FR: Farley Road Cutting and Acklands Coppice (SJ 637 026). Lower Hill Farm Track (SO 579 974).

| Lab Code | Locality Code | Depth on composite section | $\delta^{13}C$ | $\delta^{18}O$ |
|---|---|---|---|---|
| CLY082 | LQ C36 | 3.59 | 0.85 | –7.88 |
| CLY083 | LQ C34 | 4.17 | 0.86 | –5.32 |
| CLY084 | LQ C33 | 4.67 | 0.79 | –5.29 |
| CLY086 | LQ C30 | 5.63 | 1.09 | –5.01 |
| CLY087 | LQ C27 | 6.53 | 1.09 | –7.00 |
| CLY088 | LQ C26 | 7.45 | 0.84 | –5.64 |
| CLY089 | LQ C25 | 7.96 | 1.08 | –5.79 |
| CLY090 | LQ C24 | 8.89 | 1.21 | –6.10 |
| CLY091 | LQ C23 | 9.85 | 2.29 | –5.75 |
| CLY092 | LQ C22 | 10.54 | 1.51 | –8.05 |
| CLY093 | LQ C20 | 11.16 | 2.11 | –6.56 |
| CLY094 | LQ C19 | 12.20 | 2.15 | –5.55 |
| CLY095 | LQ C18 | 13.07 | 2.71 | –7.56 |
| CLY096 | LQ C17 | 13.69 | 2.58 | –8.03 |
| CLY097 | LQ C16 | 14.41 | 2.79 | –5.53 |
| CLY098 | LQ C15 | 14.92 | 2.80 | –6.55 |
| CLY099 | LQ C14 | 15.35 | 2.69 | –7.29 |
| CLY100 | LQ C13 | 15.88 | 3.16 | –5.55 |
| CLY101 | LQ C12 | 16.33 | 3.32 | –4.88 |
| CLY102 | LQ C11 | 17.06 | 2.87 | –6.21 |
| CLY103 | LQ C10 | 17.39 | 3.53 | –5.58 |
| CLY104 | LQ C9 | 17.76 | 3.28 | –5.72 |
| CLY105 | LQ C8 | 18.66 | 3.40 | –6.03 |
| CLY106 | LQ C7 | 19.18 | 3.46 | –4.56 |
| CLY107 | LQ C6 | 20.44 | 3.31 | –5.16 |
| CLY108 | LQ C5 | 20.67 | 3.58 | –5.34 |
| CLY109 | LQ C4 | 21.66 | 3.50 | –5.24 |
| CLY110 | LQ C3 | 22.13 | 3.78 | –5.52 |
| CLY111 | LQ C2 | 22.94 | 3.59 | –5.40 |
| CLY112 | LQ C1 | 23.74 | 3.38 | –6.19 |
| CRLY146 | HH1 | 25.58 | 2.12 | –6.52 |
| CRLY147 | HH2 | 25.98 | 2.13 | –5.83 |
| CRLY148 | HH3 | 26.67 | 2.31 | –5.44 |
| CRLY149 | HH4 | 27.84 | 2.31 | –5.77 |
| CRLY150 | HH5 | 29.10 | 1.92 | –6.36 |
| CRLY151 | HH6 | 29.86 | 2.19 | –6.73 |
| CRLY152 | HH7 | 30.85 | 2.16 | –6.03 |
| CRLY153 | HH8 | 32.21 | 2.30 | –7.39 |
| CRLY154 | HH9 | 33.50 | 2.16 | –6.72 |
| CRLY155 | HH10 | 34.91 | 2.23 | –6.40 |
| CRLY156 | HH11 | 34.96 | 2.34 | –6.39 |
| CRLY157 | HH12 | 34.96 | 2.31 | –5.86 |

| Lab Code | Locality Code | Depth on composite section | $\delta^{13}C$ | $\delta^{18}O$ |
|---|---|---|---|---|
| CRLY158 | HH13 | 35.12 | 2.38 | –5.69 |
| CLY113 | FR C21 | 35.33 | 2.11 | –5.75 |
| CRLY159 | HH14 | 35.39 | 1.94 | –6.39 |
| CLY114 | FR C20 | 35.62 | 2.14 | –5.78 |
| CRLY160 | HH15 | 35.79 | 2.05 | –5.84 |
| CLY115 | FR C19 | 36.02 | 2.13 | –5.48 |
| CRLY161 | HH16 | 36.34 | 2.14 | –6.66 |
| CLY116 | FR C18 | 36.56 | 2.26 | –5.32 |
| CRLY162 | HH17 | 36.71 | 2.23 | –5.73 |
| CRLY163 | HH18 | 36.80 | 2.12 | –5.70 |
| CRLY164 | HH19 | 37.14 | 2.24 | –6.20 |
| CLY118 | FR C16 | 37.30 | 2.32 | –5.92 |
| CRLY165a | HH20 | 37.36 | 2.46 | –5.96 |
| CLY119 | FR C15 | 37.49 | 1.93 | –6.61 |
| CRLY166 | HH21 | 37.86 | 2.37 | –6.29 |
| CLY120 | FR C14 | 38.03 | 1.94 | –7.20 |
| CLY117 | FR C17 | 38.13 | 0.33 | –8.17 |
| CRLY167 | HH22 | 38.29 | 2.51 | –5.78 |
| CLY121 | FR C13 | 38.37 | 2.38 | –5.80 |
| CRLY168 | HH23 | 38.46 | 2.42 | –6.17 |
| CLY251 | FR01 | 38.57 | 1.53 | –5.30 |
| CLY252 | FR02 | 38.74 | 1.42 | –5.27 |
| CLY253 | FR03 | 38.74 | 1.62 | –4.55 |
| CLY254 | FR04 | 38.89 | 1.84 | –4.77 |
| CLY255 | FR05 | 38.93 | 1.59 | –6.50 |
| CLY256 | FR06 | 38.96 | 2.00 | –4.24 |
| CLY257 | FR07 | 39.03 | 2.11 | –5.14 |
| CLY258 | FR08 | 39.12 | 2.16 | –5.73 |
| CLY259 | FR09 | 39.23 | 1.87 | –6.08 |
| CLY260 | FR10 | 39.30 | 2.22 | –6.60 |
| CLY261 | FR11 | 39.34 | 2.01 | –4.85 |
| CLY262 | FR12 | 39.62 | 2.05 | –4.85 |
| CLY263 | FR13 | 39.75 | 2.19 | –5.19 |
| CLY264 | FR14 | 39.88 | 1.93 | –6.18 |
| CLY265 | FR15 | 40.18 | 2.19 | –5.21 |
| CLY266 | FR16 | 40.22 | 2.39 | –4.77 |
| CLY267 | FR17 | 40.42 | 2.53 | –5.03 |
| CLY268 | FR18 | 40.51 | 1.93 | –6.83 |
| CLY269 | FR19 | 40.52 | 2.05 | –5.78 |
| CLY270 | FR20A | 40.62 | 2.58 | –5.10 |
| CLY271 | FR20B | 40.73 | 2.31 | –5.25 |
| CLY272 | FR21 | 40.91 | 2.04 | –5.92 |

| Lab Code | Locality Code | Depth on composite section | $\delta^{13}C$ | $\delta^{18}O$ |
|---|---|---|---|---|
| CLY273 | FR22 | 41.11 | 2.05 | –5.81 |
| CLY274 | FR23 | 41.29 | 2.57 | –5.17 |
| CLY275 | FR24 | 41.31 | 2.45 | –5.16 |
| CLY276 | FR25 | 41.72 | 2.43 | –5.25 |
| CLY277 | FR26 | 41.73 | 2.17 | –5.32 |
| CLY278 | FR27 | 42.05 | 1.50 | –4.95 |
| CLY279 | FR28 | 42.26 | 1.80 | –6.92 |
| CLY280 | FR29 | 42.38 | 2.24 | –5.54 |
| CLY281 | AC01 | 42.42 | 2.15 | –6.00 |
| CLY282 | AC02 | 42.47 | 2.42 | –6.50 |
| CLY283 | AC03 | 43.03 | 2.39 | –5.80 |
| CLY122 | FR C12 | 43.44 | 2.25 | –5.98 |
| CLY123 | FR C11 | 44.47 | 1.53 | –6.29 |
| CLY124 | FR C10 | 45.49 | 2.32 | –6.03 |
| CLY125 | FR C9 | 46.61 | 2.13 | –7.06 |
| CLY126 | FR C8 | 47.21 | 2.37 | –5.78 |
| CLY127 | FR C7 | 48.20 | 2.31 | –6.03 |
| CLY128 | FR C6 | 49.19 | 2.40 | –5.63 |
| CLY129 | FR C5 | 50.81 | 2.34 | –5.91 |
| CLY130 | FR C4 | 51.83 | 2.62 | –5.68 |
| CLY131 | FR C3 | 52.85 | 2.11 | –6.19 |
| CLY132 | FR C2 | 53.88 | 2.34 | –6.23 |
| CLY133 | FR C1 | 55.16 | 2.24 | –6.93 |
| CLY321 | ACOP106 | 55.73 | 2.17 | –7.49 |
| CLY322 | ACOP107 | 56.16 | 2.39 | –5.71 |
| CLY323 | ACOP108 | 56.43 | 2.28 | –6.88 |
| CLY324 | ACOP109 | 56.56 | 1.94 | –6.76 |
| CLY325 | ACOP110 | 56.79 | 2.26 | –6.05 |
| CLY326 | ACOP111 | 56.96 | 2.28 | –5.86 |
| CLY327 | ACOP112 | 57.12 | 1.66 | –6.64 |
| CLY328 | ACOP113 | 57.31 | 1.94 | –6.34 |
| CLY329 | ACOP114 | 57.48 | 1.29 | –6.75 |
| CLY330 | ACOP115 | 57.65 | 2.28 | –6.02 |
| CLY331 | ACOP116 | 57.81 | 2.20 | –6.12 |
| CLY332 | ACOP117 | 58.05 | 1.83 | –7.14 |
| CLY333 | ACOP118 | 58.28 | 2.29 | –6.09 |

| Lab Code | Locality Code | Depth on composite section | $\delta^{13}C$ | $\delta^{18}O$ |
|---|---|---|---|---|
| CLY334 | ACOP119 | 58.65 | 2.21 | –5.50 |
| CLY335 | ACOP120 | 58.97 | 1.89 | –7.12 |
| CLY336 | ACOP121 | 59.33 | 2.26 | –6.19 |
| CLY337 | ACOP122 | 59.68 | 2.14 | –6.35 |
| CLY338 | ACOP123 | 60.02 | 2.07 | –6.09 |
| CLY339 | ACOP124 | 60.38 | 2.14 | –6.04 |
| CLY287 | LHF101 | 66.81 | 1.63 | –6.03 |
| CLY288 | LHF102 | 67.32 | 1.61 | –6.75 |
| CLY289 | LHF103 | 67.51 | 2.58 | –5.35 |
| CLY290 | LHF104 | 67.74 | 2.58 | –5.35 |
| CLY291 | LHF105 | 67.96 | 2.54 | –4.93 |
| CLY292 | LHF106 | 68.94 | 2.54 | –5.02 |
| CLY293 | LHF201 | 69.16 | 1.68 | –7.28 |
| CLY294 | LHF202 | 69.45 | 1.20 | –6.36 |
| CLY295 | LHF203 | 69.72 | 2.55 | –5.04 |
| CLY296 | LHF204 | 70.16 | 2.03 | –6.98 |
| CLY297 | LHF205 | 72.01 | 1.97 | –5.64 |
| CLY298 | LHF301 | 72.30 | 1.91 | –5.46 |
| CLY299 | LHF303 | 72.60 | 1.96 | –5.27 |
| CLY300 | LHF304 | 72.91 | 1.09 | –6.32 |
| CLY301 | LHF305 | 73.25 | 1.58 | –6.31 |
| CLY302 | LHF306 | 73.73 | 1.15 | –6.76 |
| CLY303 | LHF307 | 74.00 | 1.09 | –6.64 |
| CLY304 | LHF308 | 74.27 | 2.13 | –6.30 |
| CLY305 | LHF401 | 76.88 | 2.38 | –5.43 |
| CLY306 | LHF402 | 77.17 | 2.35 | –7.11 |
| CLY307 | LHF501 | 78.57 | 2.39 | –6.14 |
| CLY308 | LHF502 | 78.92 | 2.39 | –6.35 |
| CLY309 | LHF503 | 79.12 | 2.20 | –6.50 |
| CLY310 | LHF601 | 80.50 | 2.11 | –6.56 |
| CLY311 | LHF602 | 80.84 | 1.74 | –7.22 |
| CLY312 | LHF603 | 81.03 | 2.27 | –6.44 |
| CLY313 | LHF604 | 81.30 | 2.15 | –6.23 |
| CLY314 | LHF605 | 81.69 | 2.21 | –6.19 |
| CLY315 | LHF606 | 82.05 | 1.70 | –7.31 |